J Fluoresc (2010) 20:105–114
DOI 10.1007/s10895-009-0528-1

ORIGINAL PAPER

On the Resolution Capabilities and Limits of Fluorescence Lifetime Correlation Spectroscopy (FLCS) Measurements

Steffen Rüttinger · Peter Kapusta · Matthias Patting · Michael Wahl · Rainer Macdonald

Received: 6 May 2009 / Accepted: 29 June 2009 / Published online: 20 August 2009

Abstract Quantitative tests were performed in order to explore the practical limits of FLCS. We demonstrate that: a) FLCS yields precise and correct concentration values from as low as picomolar to micromolar concentrations; b) it is possible to separate four signal components in a single detector setup; c) diffusion times differing only 25% from each other can be resolved by separating a two component mixture based on the different fluorescence lifetimes of both components; d) most of the inherent technical limitations of conventional FCS are easily overcome by FLCS employing a single detector channel confocal detection scheme.

Keywords Fluorescence lifetime correlation spectroscopy (FLCS) · Fluorescence correlation spectroscopy (FCS) · Single molecule detection (SMD) · Confocal laser scanning microscopy (CLSM)

Introduction

Fluorescence correlation spectroscopy (FCS) provides information about the concentration and on the dynamics of single or few molecules in a confined observation volume. Since its introduction by Magde et al. [1–3] and especially after its combination with confocal microscopy by Rigler and Widengren [4] (for overview see [5] and [6]) it has proven to be a powerful and versatile tool for biophysical research.

During the decade long history of application, however, several shortcomings have been identified:

(i) Although a single diffusion time can be measured correctly and with relatively high precision, resolving two or more species is generally difficult. The diffusion time must differ at least by a factor of 1.6 to be resolved in a two-component mixture under suitable conditions [7]. To overcome this problem e.g. for experiments measuring reaction kinetics, dual-color and two-photon cross-correlation experiments have been performed [8–17].

(ii) Unavoidable uncorrelated signal components (e.g. Raman scattering) on FCS time scales may significantly reduce the correlation amplitude and therefore introduce systematical errors that need to be corrected for. This influence is especially strong at low concentrations and for dyes of low molecular brightness. To account for this systematic error, calculation of a background correction factor [18, 19] has proven successful, as has the use of time-gated detection [20, 21].

(iii) Since the total number of photons a single molecule can emit during its life is limited, high quantum yield avalanche photodiodes operated in photon-counting (Geiger-) mode are frequently used in FCS. In counting experiments, several detector artifacts play a non-negligible role [22]. Particularly, dark counts and afterpulsing are disturbing because the former

Electronic supplementary material The online version of this article (doi:10.1007/s10895-009-0528-1) contains supplementary material, which is available to authorized users.

S. Rüttinger (✉) · R. Macdonald
Physikalisch-Technische Bundesanstalt,
Abbestr. 2-12,
10587 Berlin, Germany
e-mail: ruettinger@gmail.com

P. Kapusta · M. Patting · M. Wahl
PicoQuant GmbH,
Kekuléstr. 7,
12489 Berlin, Germany

damps the correlation amplitude whereas the latter manifests as a fast decaying component at short correlation times [23]. It is difficult, if not impossible, to account for the systematic errors caused by the dark counts and afterpulsing because of their dependence on the signal-to-background ratio and on the total count rate. Contemporary FCS detection schemes eliminate the effect of afterpulsing by cross-correlating the signal split between two independent detectors. Alternatively, the afterpulsing contribution to the resulting correlation function is approximated by a (multi-) exponential decay term during the statistical analysis (fitting) [24]. However, the effect of dark counts and scattering still has to be corrected separately.

All the common approaches to overcome the above-mentioned problems require a more complicated optical setup (experiment), at least two detectors, additional measurements, and/or the introduction of additional adjustable parameters into the analysis of the FCS results. Multiple labeling with spectrally different fluorophores may or may not be feasible. Dual-color FCS suffers from spectral cross talk and from non-ideal overlap of the confocal detection volumes. And even when perfect overlap is achieved they still would differ in size because the confocal volume depends on both, excitation and detection wavelength. Mutual influence of adjustable model parameters is a well-known, general problem in multi parameter fitting.

Fluorescence lifetime correlation spectroscopy (FLCS), first proposed in 2002 [25], is a powerful tool to solve the above-mentioned problems in a different way. In that first report, the complete mathematics behind this approach is explained and quantitative separation of the signal of two freely diffusing compounds has been demonstrated. A further step ahead is the cross-correlation of separated signal components (two labels with different lifetimes) in order e.g. to study dye exchange between unilamellar vesicles [26]. The technique has been also used to remove the effect of afterpulsing on the autocorrelation [23]. When FLCS is combined with lifetime tuning, diffusion coefficients of identical molecules in different environments can be determined simultaneously. This has been demonstrated using solid (quenching) surfaces supporting phospholipid bilayers [27]. A change of lifetime as a result of conformational change has been utilized to reveal the dynamics of DNA condensation [28, 29].

In this paper we present results which—to the best of our knowledge—prove for the first time quantitatively that FLCS yields correct and precise correlation amplitudes even in the case of very low concentrations (<50 pM), where uncorrelated background significantly hampers the extraction of correct particle numbers in conventional FCS analysis schemes. Furthermore, we show the first quantitative decomposition of the FCS curves and the resulting concentrations and diffusion times of components in a binary mixture, although both fluorophores have almost identical emission spectra and similar size. This has been achieved with a simple single color, single detector confocal setup under non-ideal conditions, where detector afterpulsing and scattered excitation light cannot be neglected. Our findings point out the resolution capabilities and limits of FLCS which are relevant for application of this method.

Method

FLCS combines standard FCS with time correlated single photon counting (TCSPC), therefore it relies on pulsed excitation instead of CW light. The primary result of an FLCS experiment is a data file containing a chronological list of detector events. These records consist of: a) an identifier of the detector that caused the event; b) the time elapsed from the start of the experiment; c) the time elapsed from the prior excitation pulse. These pieces of information will be referred to as *routing*, *time-tag* and *nanosecond-delay* (*ns-delay*), respectively, in the following.

In the conventional FCS approach the correlation function is calculated from time-tags regardless of the ns-delay. In conventional TCSPC, on the other hand, the fluorescence decay curve is obtained by histogramming the ns-delays regardless of their time-tags. FLCS analysis combines both, i.e., the information content of time-tags and ns-delays. A detailed recipe has been published in reference [30], and exact mathematical treatment can be found in references [25, 31]. Only the basic concept is outlined here.

The separation of signal components in FLCS is based on the knowledge of their characteristic TCSPC histograms, referred to as TCSPC patterns hereafter. There are various ways to obtain these patterns, and several suitable methods are described in the Results section. The TCSPC patterns of each of the individual signal components together with the total TCSPC histogram of the combined signal contributions from the whole measurement file (a primary experimental observable, always readily available after a FLCS experiment) serve as the input for the calculation of FLCS filter functions. For each signal component an associated FLCS filter is calculated, which acts as a particular weighting function upon the experimental data. For example, the detection probability of a scattered excitation photon is high during the presence of the excitation pulse but effectively zero after and before that. Hence, the filter function for scattering increases the weight of events with

the appropriate ns-delays, and decreases the weight for other delay times. A filter function for fluorescence takes into account the likelihood of scattering at short ns-delays and also the exponentially decaying detection probability of a fluorescence photon event.

The appropriate filter function applied during software correlation [32] yields the separated autocorrelation function of the selected signal component. Theoretically, a "pure" fluorescence intensity autocorrelation function can be obtained, with shape and amplitude unaffected by the above discussed unwanted contributions in this way.

Finally, it is prudent to point out the differences between the FLCS method and the older and less sophisticated time-gated FCS method [20, 21]. Time-gating, for example, excludes the scattered excitation photons by processing only events with ns-delays longer than a preset value. However, owing to the exponentially decaying behavior of fluorescence, such a time-gate unavoidably suppresses a lot of fluorescence photons at the same time, reducing the number of events that can be analyzed. In the context of FLCS, time-gating represents a binary weighting scheme: "yes", photon will be included in the correlation with a weight = 1 or "no", photon will be neglected, weight = 0). In contrast, FLCS uses a sophisticated continuous filter function to determine the contribution of each event to the selected signal component.

Experimental setup

Experiments were performed with a MicroTime 200 confocal time-resolved microscope [33, 34] based on PicoHarp 300 timing electronics (PicoQuant GmbH, Berlin, Germany) (see Supplemental Material and ref. [35]). To compare FLCS results with conventional cross-correlation analysis, the measurements were actually performed using both detectors with a 50/50 beam splitter cube between them. However, it is to be stressed, that the two detectors were solely used for validation purposes whereas FLCS does not require two detectors. During the analyses reported here the routing information was neglected (i.e. the events from different detectors summed) which is equivalent to a single detector setup. FLCS calculations were performed with the SymPhoTime software ver. 4.7.2 (PicoQuant GmbH, Berlin, Germany) and as a second independent test, with a home written MatLab (The Mathworks, Natick, MA, USA) script.

Sample preparation

Dilution series measurements described in the following were performed with the dye ATTO-655 (ATTO-TEC, Siegen, Germany) in aqueous solutions. The dye was chosen for its negligible triplet state contribution to the FCS curve [22, 36].

Samples of known dye concentration for the calibration approach were prepared as a dilution series by subsequently diluting with PBST buffer (Sigma-Aldrich) by pipetting.

For the Cy5-Atto655 mixture, pure ATTO-655 and Cy5 solutions were subsequently diluted until the particle number concentration in the confocal volume equaled approx 1. Mixtures were then prepared by mixing these two stock solutions according to the required mixing ratio.

For a more detailed description please see the Supplemental Materials.

Results and discussion

Rüttinger et al. [37, 38] investigated an ATTO-655 dilution series covering a concentration range from pM to μM by conventional FCS. The study aimed at finding the concentration range in which FCS can be used to measure diffusion coefficients and sample concentrations, and evaluated the dilution series as an alternative, model free method to precisely determine the confocal volume size. The use of the background correction factor [18] was mandatory for dye concentrations below 100 pM, but the expected concentration values have been recovered [37, 38].

For the study reported here, we investigated a similar dilution series in order to compare the previous results with the outcome of the FLCS method. A typical analysis procedure is demonstrated in the following using experimental data obtained for a 10 pM ATTO-655 solution. The outcome corresponds to one data point in Fig. 3.

The first step is the identification of the signal components. The black line in Fig. 1 shows the TCSPC histogram of the FLCS measurement. Due to the very low concentration, ATTO-655 molecules diffusing through the confocal volume are rare events. Most of the time only dark counts and scattered excitation photons are detected, resulting in the high offset (background) and the bump at the beginning of the fluorescence decay curve. Due to the high excitation repetition rate (40 MHz) in this experiment, the flat background contains also the contribution of detector afterpulsing [23, 30]. Thus our assumption is that the measured signal consists of the following five components: i) fluorescence from our target molecule; ii) scattered excitation light; iii) residual room light; iv) detector dark counts; and v) detector afterpulsing.

The second step is to obtain the pure, separated TCSPC patterns of the components. Stray room light, dark counts and afterpulses are entirely random events on the 25 ns histogram time-scale [23, 30]. They are evenly distributed

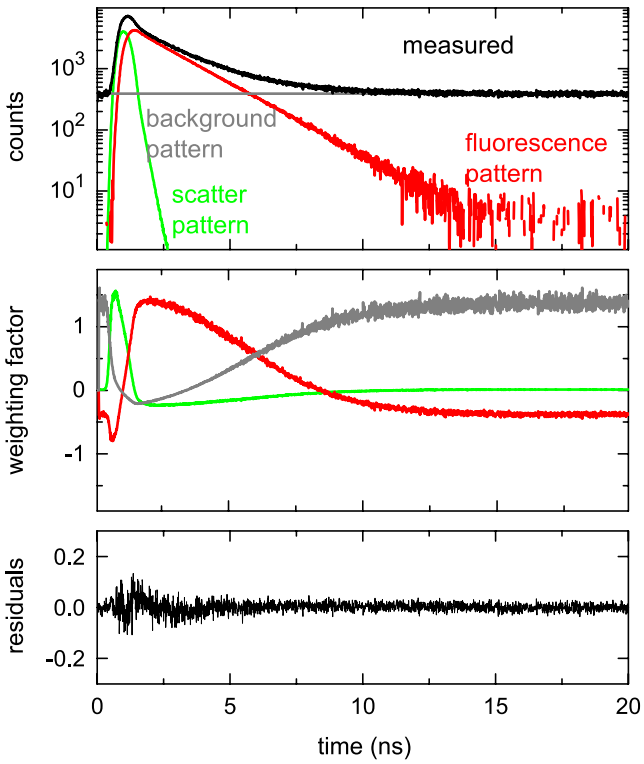

Fig. 1 TCSPC decomposition into patterns and FLCS filter functions for 10 pM ATTO-655 solution. Three distinct patterns are identified in the measured TCSPC histogram: pure fluorescence (*red*), scattering (*green*) and the sum of afterpulsing, dark counts and residual room light (*grey*). The fluorescence pattern is a background subtracted TCSPC histogram of a 100 nM ATTO-655 solution. The scattering pattern was recorded putting a mirror on top of the objective and replacing the detection bandpass filter with an OD3 filter. The 3rd pattern is a horizontal line at the average background level of the TCSPC histogram. The middle panel shows the calculated FLCS filters for these signal components. The bottom panel shows the weighted residuals of the decomposition

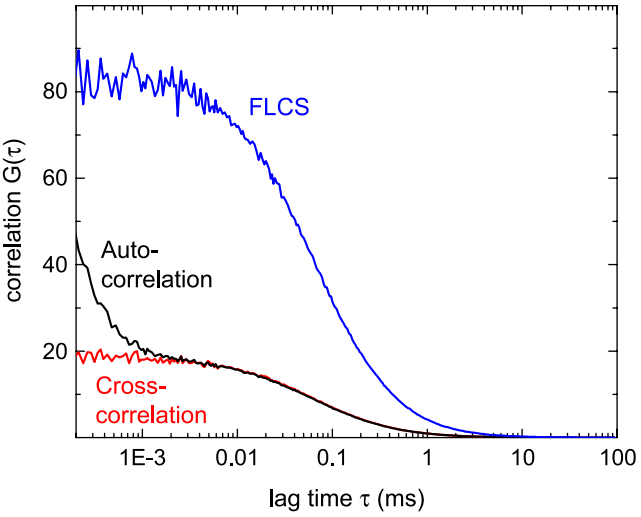

Fig. 2 Correlation functions for a 10 pM ATTO-655 solution. Comparison of conventional autocorrelation (*black*) and cross-correlation (*red*) with FLCS filtered correlation (*blue*). The blue curve corresponds to the autocorrelation of pure fluorescence intensity, thus representing the correct result

in the time span of the histogram; their common pattern is a flat line. The scattering pattern is well approximated by a background-subtracted histogram of the backscattering from a clean glass cover slip or a mirror. One gets this histogram by replacing the detection band pass filter with a suitable neutral density filter and setting the count rate to a value comparable to the signal intensity during the actual FLCS measurement. Finally, the pure fluorescence pattern can be obtained by measuring a higher concentrated solution of the same dye. For example, in a decay curve of a 100 nM ATTO-655 solution, the scattering contribution is entirely negligible. Of course, the background level is subtracted again. If the assumptions are correct, the total TCSPC histogram for any ATTO-655 concentration should be a linear combination of these three patterns.

As a quick test and a means of improving the patterns, we used a simple iterative algorithm to reconstruct the measured TCSPC histogram. The optimizer varies only the amplitudes and determines the occasional small time shifts of the normalized patterns. A representative result is shown in Fig. 1. The residuals in the bottom panel indicate that the decomposition is correct, i.e., the reconstructed histogram is virtually the same as the measured (except for the noise, of course). While this step is in fact not absolutely necessary for FLCS filter calculation, the results are very informative. The area under each scaled pattern is proportional to the fraction of the detected intensity contributed by the corresponding signal component. The total TCSPC histogram in Fig. 1 has the following composition: 44%

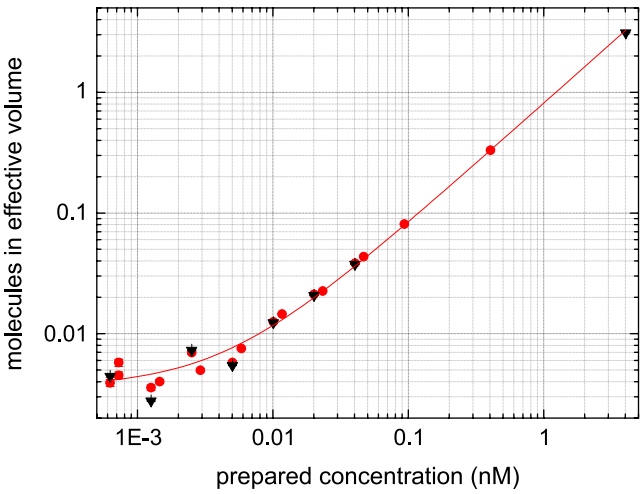

Fig. 3 Dependence of recovered particle number on prepared concentration. Red dots: FLCS results of two independent dilution series. *Black triangles*: conventional two-detector cross-correlation analysis with background correction. The *red curve* is actually a linear fit in this log-log plot

fluorescence photons, 11% scattered excitation photons, and the remaining 45% of counts belong to dark counts, residual room light and afterpulsing.

FLCS filter functions for the identified components are calculated from the same patterns and total TCSPC histogram, but the procedure now involves a matrix pseudo-inversion [25, 30, 31]. Comparison of patterns with the corresponding FLCS filters (middle panel of Fig. 1) clarifies the meaning of weighting. An event has the largest positive weight when the probability of registering it is high, and other events are unlikely at the same time. As an example, detection of a scattered excitation photon is most likely at early times. This is reflected in the filter function for this component by weights greater than 1 for ns-delays around the onset of the excitation pulse. Slightly later, fluorescence photons start to prevail. The weighting factor provided by the filter for scattering therefore decreases, whereas events with the same ns-delay receive higher weights via the fluorescence filter. A flat TCSPC pattern means ns-delay independent detection probability. However, the shape of the corresponding filter function reflects the time dependent likelihood of other possible (photon) events. It needs to be stressed that the sum of all three weighting factors always equals 1 at any ns-delay. This means that all events are equivalent, none is discarded, but a single event contribution is specially distributed between the signal components.

Using the filter function for pure ATTO-655 fluorescence (red curve in the middle panel of Fig. 1) during a software autocorrelation [32] of all events , the blue curve depicted in Fig. 2 was obtained. This is the FLCS-filtered autocorrelation function, providing the expected particle number.

Bearing in mind the composition of the detected intensity as revealed by decay curve decomposition, it is not surprising that a conventional FCS approach (i.e. simple autocorrelation of all detected events without filtering or time-gating) yields a complex correlation function (black curve in Fig. 2). Using two detectors working in parallel, we can cross-correlate their signal by making use of the routing information stored for every event. The result (red in Fig. 2) indicates that the fast decay at the beginning of the black curve was caused by detector afterpulsing. However, the cross-correlation amplitude is still damped by uncorrelated signal components. Dark counts and scattering are always uncorrelated on the lag time span of our interest. Afterpulses of one detector are completely independent of the other detector's signal, i.e. they behave as uncorrelated events in cross-correlation analysis. It is therefore possible to correct the amplitude by multiplying it with a factor of $(1+<b>/<f>)^2$ where <b> and <f> are average background and pure fluorescence detector count rates, respectively [18]. For 10 pM ATTO-655 we get a correction factor of 4.3. The *corrected* cross-correlation amplitude finally reproduces the FLCS filtered result (blue curve).

A proof that FLCS indeed yields the correct correlation amplitudes is the linear dependence of the recovered particle number on the prepared concentration in the range from as low as 2 pM up to 10 nM, as shown in Fig. 3. The red dots represent FLCS results of two independent dilution series experiments performed within 2 weeks. Patterns were recorded at the beginning of each measurement day.

Black triangles represent the outcome of conventional two-detector cross-correlation analysis of data files obtained during the second dilution series. In this case, we also performed additional blank experiments to determine the background correction factors.

Both independent analysis methods yielded the same results. We emphasize here that by using FLCS, this quantitative study did not require two detectors and any additional correction factors. Rather, only two TCSPC histograms that can be easily obtained were required.

To further demonstrate the outstanding capabilities of FLCS, we separated the autocorrelation functions of Cy5 and ATTO-655 dyes in diluted aqueous solution, under non-ideal conditions i.e. in the presence of light scattering and detector afterpulsing. These molecules are well-known fluorescence labels, popular in FCS studies. Due to their overlapping emission spectra, however, it is impossible to spectrally separate their signal contributions.

ATTO-655 and Cy5 stock solutions having an average particle number of 1 in the confocal volume were prepared. Figure 4a shows their corresponding autocorrelation curves, together with that of their 1:1 mixture (Fig. 4b). While the Cy5 correlation signal (Fig. 4a—blue curve) exhibits a pronounced off state fraction caused by cis-trans isomeration ($T \sim 30\%$), with a characteristic time of $\tau_{cis\text{-}trans}=4\,\mu s$, ATTO-655 is virtually free from isomeration kinetics and does not show triplet-like states (Fig. 4a-red curve). Both dyes show slightly different diffusion times owing to different diffusion coefficients ($D_{ATTO\text{-}655}=424\,\mu m^2/s$, $D_{Cy5}=255\,\mu m^2/s$). Note, that these diffusion constants are not resolvable in a mixture by means of a FCS model fitting [7]. Fitting a two component model to the correlation curve, the diffusion times of the two components must be fixed in order to extract the remaining parameters, i.e., extracting the diffusion times from the fit is not possible. A model assumption of single diffusing particle with a triplet term sufficiently describes the correlation curve, even though the extracted parameters are obviously false (see Fig. 4b and the supplement for a detailed discussion of the fits). For comparison the FLCS separated correlation curves of ATTO-655 and Cy5 of the 1:1 mixture are shown in Fig. 4c. Note that the separated curves are almost identical to the pure ATTO-655 and Cy5 curves (Fig. 4a). Only the

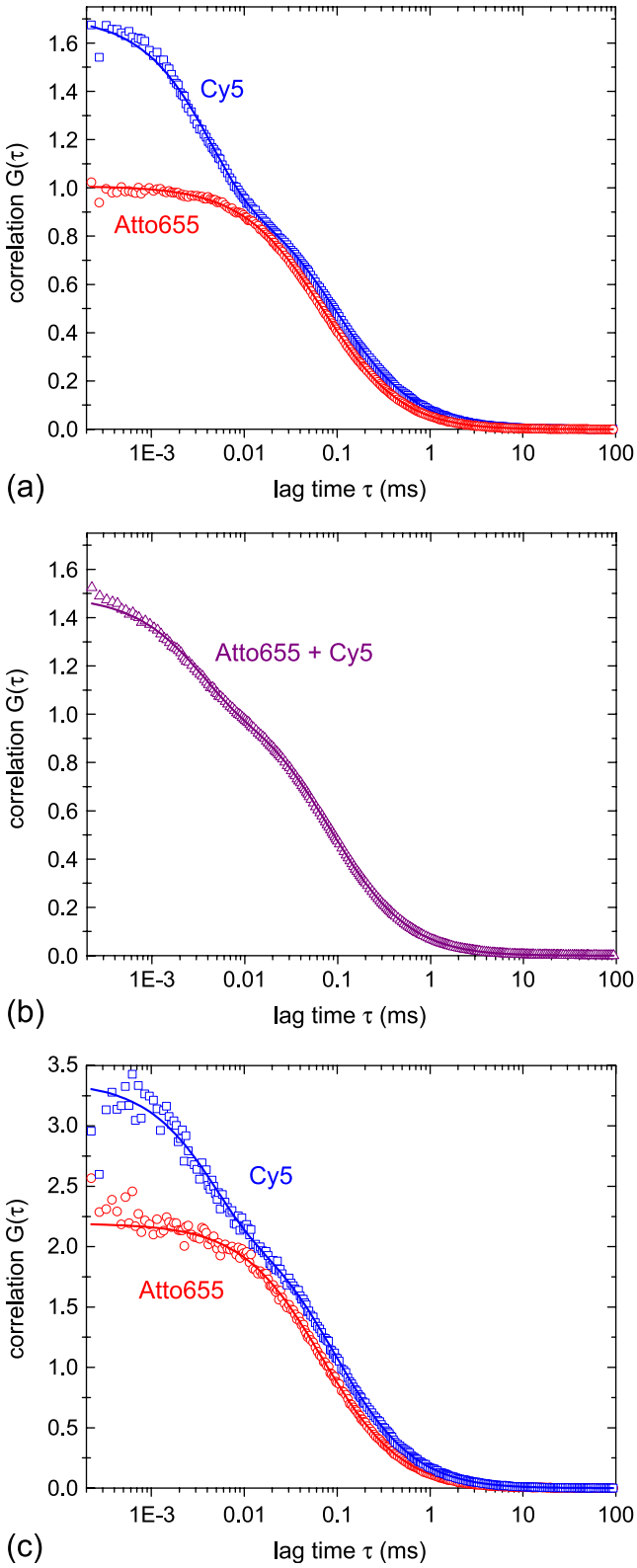

◀ **Fig. 4** **a** Correlation curves and their respective fits of the pure Cy5 and ATTO-655 stock solutions. **b** Correlation curve of a 1:1 mixture of the two stock solutions of Cy5 and ATTO-655 together with a fit of a single component diffusion model including a triplet term. Note that this model—although false—is able to reproduce the correlation curve of the mixture. **c** FLCS separated correlation curves of the same mixture give—apart from the doubled correlation amplitudes due to the halved specific concentrations—almost identical correlation curves as for the pure stock solutions depicted in (**a**). The extracted fitting parameters are listed in Table 1

correlation amplitudes have doubled as expected due to their now halved specific concentrations (see also Table 1).

In order to separate the autocorrelation functions of the components, we use the background subtracted decay curves of 100 nM solutions as pure fluorescence patterns. The scattering pattern was obtained as described above by replacing the sample with a mirror and the fluorescence bandpass by an OD3 filter (IRF method). The resulting patterns including the flat background line are shown in Fig. 5a. The amplitudes of the patterns represent their relative contribution to the measured signal. In essence, the TCSPC histogram of the mixture (black line in Fig. 5a) is reproduced quantitatively.

The separated autocorrelation functions of the identified signal components are shown in Fig. 6. Figure 6a and b prove that FLCS is indeed able to decompose the signal of a binary mixture of two spectrally irresolvable dyes in the

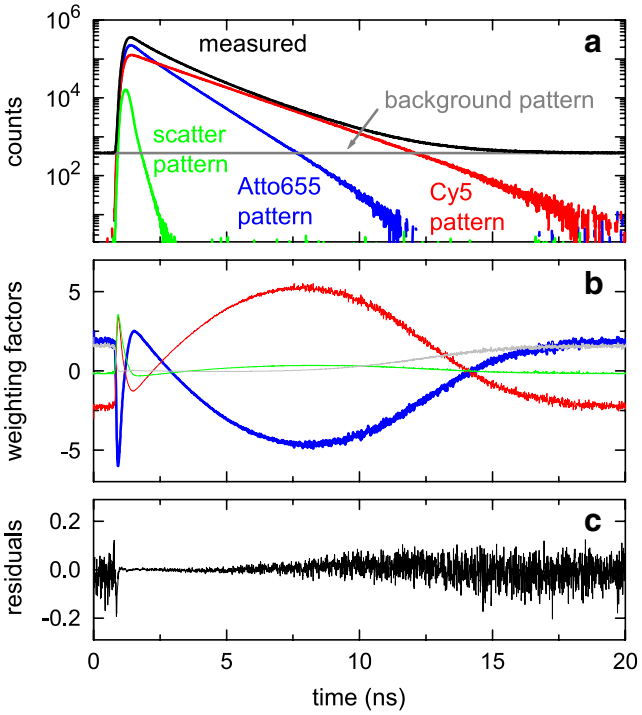

Fig. 5 Decay curve decomposition and FLCS filters for a 1:1 Cy5 and ATTO-655 mixture. **a** Scaled patterns of the four signal components (ATTO-655: *red*, Cy5: *blue*, light scattering: *green*, background plus afterpulsing: *grey*) and the TCSPC histogram of the measurement (*black*). The scaling factors of the normalized patterns represent their respective contributions to the measured TCSPC curve (*black line*): 48.5% Cy5, 48.5% ATTO-655, 0.8% Scattering, 2.2% background and afterpulsing. **b** Filter curves for these signal components. **c** Residuals indicating that the four chosen patterns are able to reconstruct the measured histogram of (**a**)

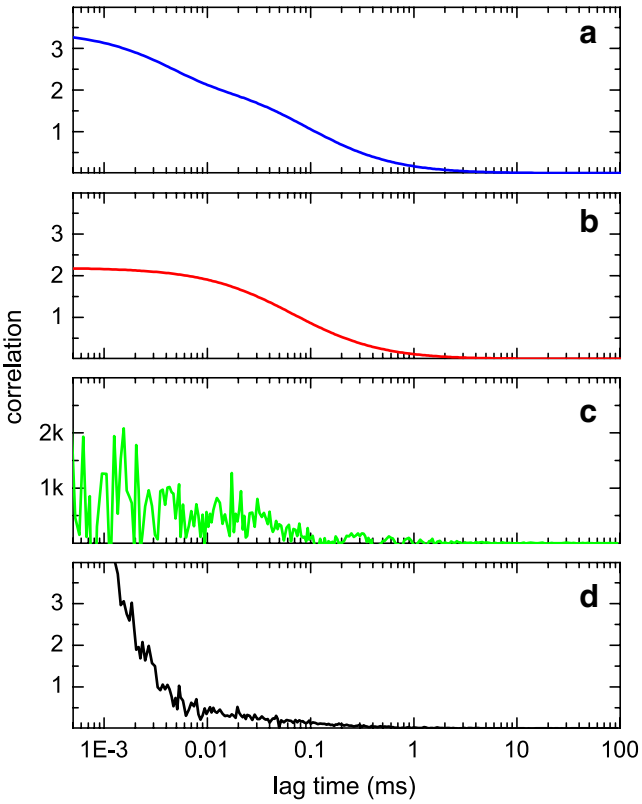

Fig. 6 FLCS filtered correlation functions of the identified signal components in the 1:1 mixture of diluted Cy5 and ATTO-655. **a** Cy5, **b** ATTO-655, **c** scattering, **d** afterpulsing, dark counts and residual stray light. Note that the amplitudes of both fluorescence components (triplet corrected in the case of Cy5) equal half of the amplitudes of the pure components shown in Fig. 4, as expected for a 1:1 mixture

presence of other, unwanted contributions, as long as their TCSPC patterns differ. Figure 6c and d serve as a test to ascertain that the decomposition was successful. Ideally, the scattering signal should be completely uncorrelated due to the high number of water molecules causing the scattering. However, we observed a residual correlation even for the decomposed scattering part of the signal with a characteristic time in the range of the diffusion times of the dye molecules. Apparently, a small fraction of fluorescence photons are falsely assigned to the scattering contribution. The correlation amplitude, however, is three orders of magnitude higher than that of the two fluorescence components (Fig. 6a and b,) and the introduced error is therefore very small. This observation is a result of the statistical nature of the weighting schemes (filters), and can be regarded as a time domain analogy of the spectral cross talk. Figure 6d displays another advantage of FLCS, showing the detector afterpulsing dynamics extracted by this method. Parameters of the measuring setup such as system dead time and detector afterpulsing probability can be extracted from this correlation curve, but this goes beyond the scope of this article.

We have repeated the above FLCS procedure for mixtures with a varying ratio of Cy5 and ATTO-655 molecules, keeping the overall concentration constant (c = 1 molecule/confocal volume). Figure 7 shows the results. The diagonal lines indicate the expected findings according to the prepared mixture while the data points are particle numbers retrieved by FLCS. The error bars are estimations based on repeated measurements. (Several mixtures were measured more than three times.) Figure 7 also reflects the expected (see Supplemental Materials) degradation of Cy5 manifested as a decrease in concentration with time (Cy5 concentration for the 0.75 mixture) when measured consecutively.

Once the autocorrelation functions of each dye component are separated as described above, it is possible to recover their diffusion parameters by standard model fitting. Figure 8 summarizes the result. The autocorrelation function of ATTO-655 has a simple shape, indicating that the model of single particle diffusion is sufficient. Consequently, the recovered diffusion times for this dye are quite precise. The larger uncertainty of Cy5 parameters is expected taking into account the need to consider an additional cis-trans isomeration term in the fit model. However, Fig. 8 proves that resolving a diffusion time difference as small as 25% is feasible using FLCS.

Conclusions and outlook

The results discussed in this paper demonstrate the robustness of FLCS in comparison to conventional FCS. Efficient use of the TCSPC information allowed

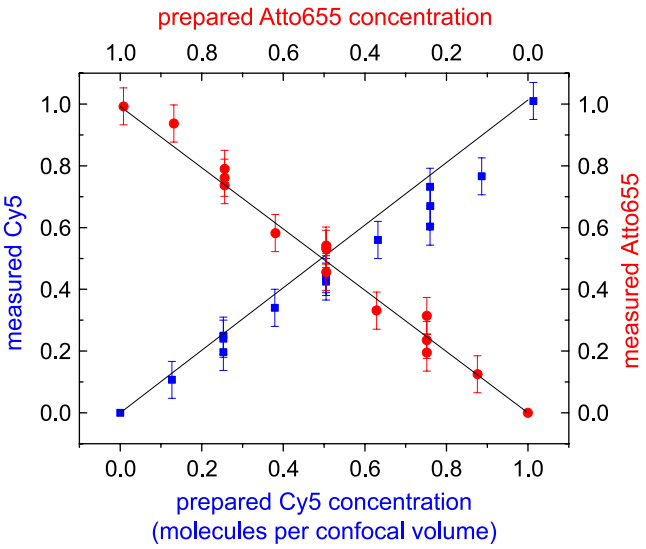

Fig. 7 FLCS separation of Cy5 and ATTO-655 for a varying concentration ratio mixture of both. The overall concentration was kept constant. The *black lines* indicate the expected concentration

Table 1 Parameters extracted by fitting diffusion models to the correlation curves shown in Fig. 4

Parameter	Pure Cy5	Pure Atto665	50:50 mixture		
			Unfiltered	Cy5 filtered	Atto655 filtered
N	1.01±0.02	0.990±0.002	0.929±0.004	0.44±0.01	0.456±0.002
τ (ms)	0.0976±0.0009	0.0702±0.0003	0.081±0.0003	0.093±0.001	0.0688±0.0007
κ	7.4±0.3	5.7±0.1	5.98±0.07	6.4±0.2	5.5±0.2
T	0.420±0.007		0.2796±0.0002	0.33±0.02	
$\tau_{cis\text{-}trans}$ (ms)	0.00417±0.00008		0.0030±0.0001	0.0043±0.0003	

us to overcome most of the inherent limitations of FCS. We have shown that common sources of errors like detector afterpulsing and/or scattered light can be dramatically reduced—if not avoided completely—by the FLCS method applied.

We presented an example in which a complete, quantitative separation of four signal components was achieved using only a single excitation wavelength and a single detector line. Even taking into account the efforts and needs to perform TCSPC, the simplicity of such method is in striking contrast to the complexity of advanced FCS setups based e.g. on dual-color FCS, alternating laser excitation, etc., heretofore employed to solve similar problems. Multicolor excitation/detection schemes always suffer from problems related to non-ideal confocal volume overlap or spectral cross talk. FLCS is limited only by the similarity of the TCSPC patterns.

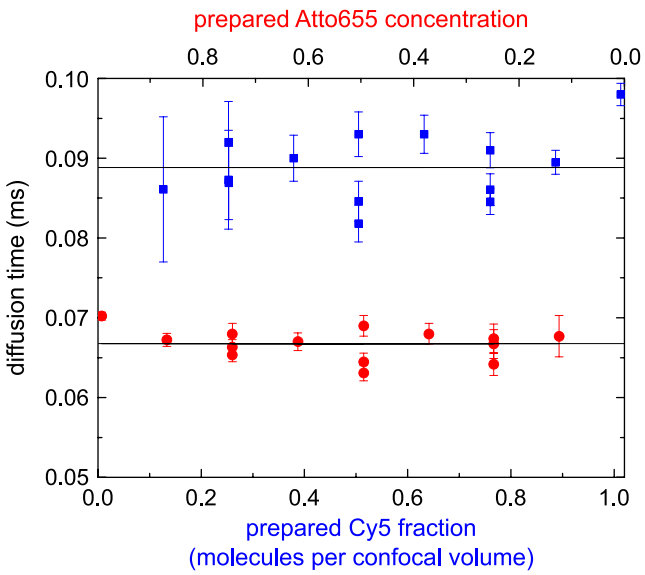

Fig. 8 Recovered diffusion times of Cy5 and ATTO-655 at various mixing concentration ratios. Note that the diffusion times to be resolved differ only by 25%

Because the signal separation in FLCS is based on temporal features and information of the signals provided by TCSPC, this method can be used to study complex multi-component samples where spectral separation of the components is difficult (e.g. due to strong spectral overlap leading to cross talk in the detector channels) or impossible (two forms or environments of the same fluorophore).

In contrast to dual-color cross-correlation experiments, FLCS also allows cross-correlation experiments with perfectly overlapping and exactly the same size (since there is only one) confocal volumes.

The demonstrated power and accuracy of FLCS offers a multitude of biologically very interesting experiments that may greatly benefit from the virtues of this method. It is, for example not necessary, to have precise prior experimental knowledge about patterns that contribute to the measured signal. Coarse assumptions about the temporal (on the ns-timescale) behavior of the different signal components might already be sufficient, e.g. to measure the relative concentrations of a binary system with two distinct fluorescence lifetimes. The two lifetime components needed could be estimated with a two-component lifetime fit. The resulting theoretic patterns from this fit model can then be used instead of experimentally determined patterns to separate the two contributions to the correlation. One might also envision using FLCS to oppress cellular background fluorescence by only calculating the correlation for the fluorescence lifetime expected from the target fluorophore. Another option is to take advantage of the change in fluorescence lifetime of several commonly used dyes induced by changes in polarity of their neighborhood, e.g., to separate membrane diffusion from free diffusion.

Acknowledgements We gratefully acknowledge financial support from the German ministry of Education and Research (BMBF, Biophotonik Project 13N8850) and the German ministry of Economics (BMWi, grant MNPQ 12/06).

References

1. Magde D, Elson EL, Webb WW (1972) Thermodynamic fluctuations in a reacting system & measurement by fluorescence correlation spectroscopy. Phys Rev Lett 29(11):705–708. doi:10.1103/PhysRevLett.29.705
2. Elson EL, Magde D (1974) Fluorescence correlation spectroscopy: I. conceptual basis and theory. Biopolymers 13:1–27. doi:10.1002/bip.1974.360130102
3. Magde D, Elson EL, Webb WW (1974) Fluorescence correlation spectroscopy: II. An experimental realization. Biopolymers 13:29–61. doi:10.1002/bip.1974.360130103
4. Rigler R, Widengren J (1990) Ultrasensitive detection of single molecules by fluorescence correlation spectroscopy. Bioscience 3:180–183
5. Thompson NL (1991) Topics in fluorescence spectroscopy, vol 1. Plenum, New York, p 337
6. Widengren J, Mets Ü (2002) In: Zander C, Enderlein J, Keller RA (eds) Wiley-VCH, ISBN3-527-40310-8, pp 69–120
7. Meseth U, Wohland T, Rigler R, Vogel H (1999) Resolution of fluorescence correlation measurements. Biophys J 76(3):1619–1631. doi:10.1016/S0006-3495(99)77321-2
8. Schwille P, Meyer-Almes FJ, Rigler R (1997) Dual-color fluorescence cross-correlation spectroscopy for multicomponent diffusional analysis in solution. Biophys J 72(4):1878–1886. doi:10.1016/S0006-3495(97)78833-7
9. Schwille P, Bieschke J, Oehlenschlager F (1997) Kinetic investigations by fluorescence correlation spectroscopy: the analytical and diagnostic potential of diffusion studies. Biophys Chem 66(2-3):211–228. doi:10.1016/S0301-4622(97)00061-6
10. Rigler R, Földes-Papp Z, Meyer-Almes FJ, Sammet C, Volcker M, Schnetz A (1998) Fluorescence cross-correlation: a new concept for polymerase chain reaction. J Biotechnol 63(2):97–109. doi:10.1016/S0168-1656(98)00079-0
11. Kettling U, Koltermann A, Schwille P, Eigen M (1998) Real-time enzyme kinetics monitored by dual-color fluorescence cross-correlation spectroscopy. Proc Natl Acad Sci USA 95(4):1416–1420. doi:10.1073/pnas.95.4.1416
12. Koltermann A, Kettling U, Bieschke J, Winkler T, Eigen M (1998) Rapid assay processing by integration of dual-color fluorescence cross-correlation spectroscopy: high throughput screening for enzyme activity. Proc Natl Acad Sci USA 95 (4):1421–1426. doi:10.1073/pnas.95.4.1421
13. Winkler T, Kettling U, Koltermann A, Eigen M (1999) Confocal fluorescence coincidence analysis: an approach to ultra high-throughput screening. Proc Natl Acad Sci USA 96(4):1375–1378. doi:10.1073/pnas.96.4.1375
14. Heinze KG, Koltermann A, Schwille P (2000) Simultaneous two-photon excitation of distinct labels for dual-color fluorescence crosscorrelation analysis. Proc Natl Acad Sci USA 97(19):10377–10382. doi:10.1073/pnas.180317197
15. Bieschke J, Giese A, Schulz-Schaeffer W, Zerr I, Poser S, Eigen M, Kretzschmar H (2000) Ultrasensitive detection of pathological prion protein aggregates by dual-color scanning for intensely fluorescent targets. Proc Natl Acad Sci USA 97(10):5468–5473. doi:10.1073/pnas.97.10.5468
16. Medina MA, Schwille P (2002) Fluorescence correlation spectroscopy for the detection and study of single molecules in biology. Bioessays 24(8):758–764. doi:10.1002/bies.10118
17. Kohl T, Heinze KG, Kuhlemann R, Koltermann A, Schwille P (2002) A Protease assay for two-photon crosscorrelation and FRET analysis based solely on fluorescent proteins. Proc Natl Acad Sci USA 99 (19):12161–12166. doi:10.1073/pnas.192433499
18. Koppel D (1974) Statistical accuracy in fluorescence correlation spectroscopy. Phys Rev A 10:1938–1945
19. Rüttinger S (2006) Confocal microscopy and quantitative single molecule techniques for metrology in molecular medicine. PhD thesis, TU-Berlin
20. Lamb DC, Schenk A, Röcker C, Scalfi-Happ C, Nienhaus GU (2000) Sensitivity enhancement in fluorescence correlation spectroscopy of multiple species using time-gated detection. Biophys J 79:1129–1138. doi:10.1016/S0006-3495(00)76366-1
21. Lamb DC, Müller BK, Bräuchle CH (2005) Enhancing the sensitivity of fluorescence correlation spectroscopy by using time-correlated single photon counting. Curr Pharm Biotechnol 6:405–414. doi:10.2174/138920105774370625
22. Höbel M, Ricka J (1994) Dead-time and afterpulsing correction in multiphoton timing with nonideal detectors. Rev Sci Instrum 65 (7):2326–2336. doi:10.1063/1.1144684
23. Enderlein J, Gregor I (2005) Using fluorescence lifetime for discriminating detector afterpulsing in fluorescence correlation spectroscopy. Rev Sci Instrum 76:033102. doi:10.1063/1.1863399
24. Zhao M, Jin L, Chen B, Ding Y, Ma H, Chen D (2003) Afterpulsing and its correction in fluorescence correlation spectroscopy experiments. Appl Opt 42(19):4031–4036. doi:10.1364/AO.42.004031
25. Böhmer M, Wahl M, Rahn H-J, Erdmann R, Enderlein J (2002) Time-resolved fluorescence correlation spectroscopy. Chem Phys Lett 353:439–445. doi:10.1016/S0009-2614(02)00044-1
26. Benda A, Hof M, Wahl M, Patting M, Erdmann R, Kapusta P (2005) TCSPC upgrade of a confocal FCS microscope. Rev Sci Instrum 76:33106. doi:10.1063/1.1866814
27. Benda A, Fagulová V, Deyneka A, Enderlein J, Hof M (2006) Fluorescence lifetime correlation spectroscopy combined with lifetime tuning: New perspectives in supported phospholipid bilayer research. Langmuir 22:9580–9585. doi:10.1021/la061573d
28. Humpolíčková J, Benda A, Sykora J, Macháň R, Kral T, Gasinska B, Enderlein J, Hof M (2008) Equilibrium dynamics of spermine-induced plasmid DNA condensation revealed by fluorescence lifetime correlation spectroscopy. Biophys J 94:L17–L19. doi:10.1529/biophysj.107.122408
29. Humpolícková J, Beranová L, Stepánek M, Benda A, Procházka K, Hof M (2008) Fluorescence lifetime correlation spectroscopy reveals compaction mechanism of 10 and 49 kbp DNA and differences between polycation and cationic surfactant. J Phys Chem B 112:16823–16829
30. Kapusta P, Wahl M, Benda A, Hof M, Enderlein J (2007) Fluorescence lifetime correlation spectroscopy. J Fluoresc 17:43–48. doi:10.1007/s10895-006-0145-1
31. Gregor I, Enderlein J (2007) Time-resolved methods in biophysics. Fluorescence lifetime correlation spectroscopy. Photochem Photobiol Sci 6:0013–0018
32. Wahl M, Gregor I, Patting M, Enderlein J (2003) Fast calculation of fluorescence correlation data with asynchronous time-correlated single-photon counting. Opt Express 11:3583–3591
33. Koberling F, Krämer B, Tannert S, Rüttinger S, Ortmann U, Patting M, Wahl M, Ewers B, Kapusta P, Erdmann R (2008) Recent advances in time-correlated single-photon counting. Proceedings of SPIE, 6862:686209
34. Wahl M, Koberling F, Patting M, Rahn H, Erdmann R (2004) Time-resolved confocal fluorescence imaging and spectroscopy system with single molecule sensitivity and sub-micrometer resolution. Curr Pharm Biotechnol 5:299–308. doi:10.2174/1389201043376841
35. Wahl M, Rahn H, Gregor I, Erdmann R, Enderlein J (2007) Dead-time optimized time-correlated photon counting instrument with synchronized, independent timing channels. Rev Sci Instrum 78:033106. doi:10.1063/1.2715948
36. Dertinger T, Pacheco V, von der Hocht I, Hartmann R, Gregor I, Enderlein J (2007) Two focus fluorescence correlation spectroscopy: a new tool for accurate and absolute diffusion

measurements. ChemPhysChem 8:433–443. doi:10.1002/cphc.200600638
37. Rüttinger S, Buschmann V, Krämer B, Erdmann R, Macdonald R, Koberling F (2007) Determination of the confocal volume for quantitative fluorescence correlation spectroscopy. Proceedings of SPIE 6630:66300D
38. Rüttinger S, Buschmann V, Krämer B, Erdmann R, Macdonald R, Koberling F (2008) Comparison and accuracy of methods to determine the confocal volume for quantitative fluorescence correlation spectroscopy. J Microsc 232(2):334–352
39. http://www.atto-tec.com/ATTO-TEC.com/Products/ATTO655_1.html